

1 **Revision 2**

2 **Discreditation of diomignite and its petrologic implications**

3 **ALAN J. ANDERSON**

4 Department of Earth Sciences, St. Francis Xavier University, Antigonish, Nova Scotia,
5 B2G 2W5 Canada

6 **ABSTRACT**

7 Diomignite ($\text{Li}_2\text{B}_4\text{O}_7$) is discredited as a mineral species, and this discreditation has been
8 approved by the International Mineralogical Association, Commission on New Minerals,
9 Nomenclature and Classification. Diomignite was originally reported to occur in virtually every
10 crystal-rich inclusion in spodumene from the Tanco pegmatite in southeastern Manitoba,
11 Canada. However, detailed study of 30 randomly selected crystal-rich inclusions in the
12 purported type material deposited at the U.S. National Museum of Natural History, 30 inclusions
13 in the purported type material from the American Museum of Natural History, and several
14 hundred inclusions in self-collected samples reveals that diomignite is absent in every inclusion
15 examined. Because no holotype specimen exists, and no neotype sample was provided by the
16 surviving authors of the original description, the presence of diomignite could not be validated.
17 The evidence provided in the original description to the IMA in 1984 is shown to be insufficient
18 to support the existence of diomignite as a mineral species.

19 The previously reported boron-rich (12 mass% B_2O_3) composition of the melt
20 represented as crystal-rich inclusions in spodumene and petalite from the Tanco pegmatite was
21 predicated on the assumption that diomignite is a common daughter mineral that occurs in most
22 inclusions and that the inclusions are primary melt inclusions. The nonexistence of diomignite,
23 and the absence of other borate daughter minerals, in these crystal-rich inclusions indicates that
24 the boron content was greatly overestimated and so comparisons to experimentally generated

25 boron-rich (>10 mass% B₂O₃) boundary-layer melts are unwarranted. Furthermore, the
26 discreditation of diomignite negates the inferred role of a Li₂B₄O₇-flux-rich melt in the
27 generation of primary pegmatite textures and rare element oxide mineralization in the Tanco
28 pegmatite. The common mineral assemblage within the crystal-rich inclusions in secondary and
29 primary spodumene can be formed by the interaction of an aqueous carbonic fluid with the
30 spodumene host.

31 **Keywords:** Diomignite, discreditation, pegmatite, inclusions, boron, internal evolution

32 INTRODUCTION

33 London et al. (1987) reported diomignite (Li₂B₄O₇) as a new mineral from the Tanco
34 pegmatite in southeastern Manitoba, Canada. It was the first mineral species to be described
35 solely as a daughter mineral in fluid inclusions, following approval in 1984 (IMA 84-58) by the
36 International Mineralogical Association, Commission on New Minerals and Mineral Names,
37 currently Commission on New Minerals, Nomenclature and Classification (CNMNC). Detailed
38 examination of several hundred spodumene-hosted inclusions from the Tanco pegmatite shows
39 that the evidence presented in the original description of diomignite is insufficient to warrant
40 valid mineral species status. Discreditation of diomignite was officially approved by the
41 CNMNC in January 2016 (decision 15-H), and reported in Hålenius et al. (2016). This paper
42 reviews the lines of evidence presented in the original description and calls into question the
43 origin of the crystal-rich inclusions (London 2008), the estimated composition of the entrapped
44 fluid (London 1986), and the inferred role of a Li₂B₄O₇ flux-rich melt in the internal evolution of
45 the Tanco pegmatite (London 1985, 1986) and the alteration of the walls rocks (Morgan and
46 London 1987; London 2008).

47 OCCURRENCE

48 Diomignite was reported to be part of an assemblage of daughter minerals that includes
49 albite, cookeite, quartz, pollucite-analcime solid solution, a microlite-group mineral and an
50 unidentified carbonate mineral within spodumene-hosted fluid inclusions from the Tanco
51 pegmatite, Manitoba, Canada. According to London et al. (1987), “*Diomignite has been*
52 *observed only as small ($\leq 30 \mu\text{m}$) anhedral to euhedral crystals in fluid inclusions in spodumene,*
53 *and tentatively in fluid inclusions in the petalite from which most of the spodumene formed. In*
54 *these associations, diomignite is an abundant and widely distributed phase; it occurs in virtually*
55 *every crystal-rich inclusion in spodumene.*” However, examination of several hundred of the
56 same type of inclusions in self-collected samples, and in 30 crystal-rich inclusions in samples
57 deposited as type material at the U.S. National Museum of Natural History, and in 30 inclusions
58 in samples deposited as type material at the American Museum of Natural History, shows that
59 most inclusions contain only quartz, zabuyelite, cookeite and a low salinity aqueous or aqueous
60 carbonic fluid (see supplemental material). Despite an exhaustive search, no inclusions were
61 shown to contain crystals of lithium tetraborate.

62 Thomas and Davidson (2010) reported a second occurrence of diomignite in beryl-hosted
63 fluid inclusions from the Muiane pegmatite, Mozambique, but referred to the compound as
64 $\text{Li}_2\text{B}_4\text{O}_7 \cdot 5\text{H}_2\text{O}$. This second discovery was acknowledged by London (2015). However, the
65 Raman spectrum used to identify this phase does not match the spectrum of anhydrous $\text{Li}_2\text{B}_4\text{O}_7$
66 (Paul and Taylor 1982; Gorelik et al. 2003; Burak et al. 2006, Wan et al. 2014). The reported
67 vibrational frequencies (390, 446, 544, 1028, 1097, 1352 cm^{-1}), however, closely match
68 $\text{Li}_2\text{B}_4\text{O}_7 \cdot 3\text{H}_2\text{O}$. Rainer Thomas (pers. comm. 2015) has since retracted this report. The Raman
69 spectrum of the phase reported as $\text{Li}_2\text{B}_4\text{O}_7 \cdot 5\text{H}_2\text{O}$ was not saved by Thomas and Davidson, and R.
70 Thomas was unable to obtain a duplicate spectrum from the same beryl-hosted inclusions. The

71 report of diomignite or a hydrated lithium tetraborate in the inclusions from the Muiane
72 pegmatite should therefore be disregarded.

73 **TYPE MATERIAL**

74 Material purported to be type specimens of diomignite was deposited in the Smithsonian
75 Institution, National Museum of Natural History (USNM 164236), Washington, D.C., and the
76 American Museum of Natural History (AMNH 98989 and 98990) in the form of fragments and
77 doubly polished wafers of spodumene from the Tanco pegmatite, Manitoba (London et al. 1987).
78 These representative samples of spodumene were purported to be replete with diomignite-
79 bearing inclusions (London et al. 1987). However, these samples were not used to characterize
80 all of the properties reported in the original description and therefore cannot be regarded as true
81 type specimens. Because no true holotype, or cotype, sample of diomignite exists, a request for a
82 neotype specimen was made in the proposal for discreditation. No neotype specimen was
83 produced by the principal author of the original description.

84 **OPTICAL PROPERTIES**

85 Table 1 in London et al. (1987) lists the refractive indices $\omega=1.612(1)$ and $\epsilon=1.554(2)$
86 obtained from synthetic lithium tetraborate crystallized at 600 °C and 200 MPa P(H₂O).
87 However, only an averaged refractive index of $n \sim 1.6$ is reported for diomignite. According to
88 London et al. (1987), diomignite is readily recognized in doubly polished plates of spodumene
89 by its high birefringence, and where diomignite and an unidentified carbonate mineral coexist,
90 the carbonate usually can be distinguished by its higher birefringence. However, about 3 percent
91 of spodumene-hosted inclusions contain two or more crystals of zabuyelite (e.g., Figure 1) that
92 commonly display different relief and retardation due to differences in their thickness and
93 orientation within the inclusion. Raman spectroscopic analyses of several hundred high-

94 birefringence daughter minerals in the spodumene-hosted fluid inclusions indicate that they are
95 zabuyelite, or very rarely calcite or nahcolite.

96 **MORPHOLOGY**

97 Morphological and optical properties are among the main features used to identify solids
98 in unopened fluid inclusions. According to London et al. (1987), euhedral crystals of diomignite
99 commonly appear as pseudorhomboidal or pseudocubic forms. However, when crystal
100 drawings of zabuyelite are generated by SHAPE (Dowty 2000) using only simple first-order
101 pyramids and prisms, and are viewed down the c-axis, the crystals display pseudo-cubic or
102 pseudo-hexagonal outlines (Figures 2a and 2b, respectively). It is therefore suggested that
103 zabuyelite, a common and widespread daughter mineral in spodumene-hosted inclusions
104 (Anderson et al. 2001), was misidentified by London et al. (1987) as diomignite. The only SEM
105 image of a crystal purported to be diomignite is shown in London et al. (1987, Fig. 1C),
106 however, the illustrated sample was not submitted as type material, and therefore could not be
107 analyzed by Raman spectroscopic or electron microprobe techniques.

108 **CHEMICAL DATA**

109 London et al. (1987) unsuccessfully attempted to chemically analyze daughter crystals
110 they believed to be diomignite using a SIMS microprobe. Even though modern microanalytical
111 techniques such as EMPA, SIMS and LA-ICP-MS are now used for quantitative analysis of
112 boron and lithium, a chemical analysis of diomignite has still never been made. The presence of
113 Li, B and O was inferred by London et al. (1987) on the basis of filtered energy dispersive
114 analysis of daughter minerals in opened fluid inclusions. The detector employed at the time of
115 the original description was incapable of detecting light elements (i.e., $Z < 11$) and the spectra
116 obtained by London et al. (1987) showed no X-ray emission lines, indicating the mineral consists

117 wholly of elements with an atomic number of less than 11. This evidence is consistent with
118 zabuyelite (Li_2CO_3) which consists wholly of light elements and is found in almost every crystal-
119 rich inclusion (Anderson et al. 2001).

120 **X-RAY DIFFRACTION DATA**

121 Single crystal-structure data were not provided in the original description. According to
122 London et al. (1987), confirmation of the identity of diomignite was based on two faint Gandolfi
123 X-ray diffraction patterns obtained from one crystal. That crystal could not be reexamined and
124 was not included as type material because, as reported in London et al. (1987), it “had popped
125 off” the glass whisker mount and was lost.

126 Eleven of the x-ray diffraction lines obtained from the lost crystal closely match the
127 powder XRD lines obtained from synthetic $\text{Li}_2\text{B}_4\text{O}_7$ crystals synthesized at 600 °C and 200 MPa
128 $\text{P}(\text{H}_2\text{O})$ (London et al. 1987). However, without the original daughter crystal, or the XRD
129 pattern of a suitable replacement of known provenance, the XRD evidence presented by London
130 et al. (1987) does not pass sufficient rigor to be regarded as unambiguous.

131 **SOLUBILITY DATA AND PHASE RELATIONS**

132 According to London et al. (1987), diomignite can be distinguished from high
133 birefringence carbonate minerals in fluid inclusions by differences in solubility. The carbonate
134 phase is said to dissolve between 275 and 300°C while diomignite is said to dissolve at a
135 temperature of about 420°C. In most inclusions, however, the carbonate phase (i.e., zabuyelite)
136 persists well above the liquid-vapor homogenization temperature (*ca.* 312°C) to various
137 temperatures of inclusion decrepitation ($> 400^\circ\text{C}$). This indicates that the delimiting solubility
138 evidence used in the original description is incorrect.

139 If solid lithium tetraborate did exist in an aqueous fluid inclusion, it would most likely
140 occur as a hydrated species. According to the investigations of Dukelski (1906), Reburn and
141 Gale (1955), and Touboul and Bétourné (1996), the stable lithium borate in the system $\text{Li}_2\text{B}_4\text{O}_7$ -
142 H_2O at low temperature is $\text{Li}_2\text{B}_4\text{O}_7 \cdot 3\text{H}_2\text{O}$, not anhydrous $\text{Li}_2\text{B}_4\text{O}_7$.

143 London (1986) suggested that phase relations in the synthetic system LiAlSiO_4 -
144 $\text{NaAlSi}_3\text{O}_8$ - SiO_2 - $\text{Li}_2\text{B}_4\text{O}_7$ - H_2O are closely analogous to the natural fluid represented by the
145 inclusions in spodumene from Tanco. However, this comparison does not take into account the
146 strong effect that Li_2CO_3 , a major component, exerts on the microthermometric behavior of the
147 spodumene-hosted inclusions. Any broad similarities in phase relations between the zabuyelite-
148 bearing inclusions and the modeled synthetic system LiAlSiO_4 - $\text{NaAlSi}_3\text{O}_8$ - SiO_2 - $\text{Li}_2\text{B}_4\text{O}_7$ - H_2O
149 must therefore be regarded as coincidental.

150 Heating silicate-rich fluid inclusions under confining pressure will normally produce a
151 liquid that can be quenched to glass plus an aqueous solution regardless of the origin of the
152 contained solids (i.e., daughter mineral, alteration phase, or accidentally trapped mineral) (Bodnar
153 and Student 2006). Although the contents of some crystal-rich inclusions in spodumene may be
154 melted and then quenched to form glass beads plus aqueous fluid, the formation of glass is not
155 unequivocal evidence that the daughter mineral assemblage represents the products of an
156 entrapped silicate melt (Anderson 2013).

157 **RAMAN SPECTROSCOPIC ANALYSIS**

158 The application of Raman microprobe to the analysis of fluid inclusions was described by
159 Rosaco and Roedder (1979). Although *in situ* Raman spectroscopic analysis is an effective
160 technique for identifying borates in unopened fluid inclusions (e.g., Peretyazhko et al. 2000;
161 Thomas and Davidson 2010), it was not employed in the description of diomignite in 1984. In

162 this study, Dilor X-Y and LAB RAM HR microprobes were respectively used to collect spectra
163 from crystal-rich inclusions in the type samples, USNM 164236 and AMNH 98090 (see
164 supplemental material), and from several hundred inclusions in self-collected samples (Anderson
165 et al. 2001). Each spectrum represents three, thirty-second accumulations using an excitation of
166 514.5 or 532 nm. The source laser power was 180 mW.

167 Twenty-nine of the thirty inclusions examined in AMNH 98090 contain an assemblage of
168 minerals consisting of quartz, zabuyelite and a phyllosilicate (cookeite). None of the inclusions
169 were shown to contain a lithium tetraborate crystal. The phyllosilicate found in most inclusions
170 occurs as thin sheets or plumose aggregates (e.g., S98090-4e in the supplemental material) and
171 shows moderate relief and low interference colors. Some Raman spectra display a weak band at
172 266 cm^{-1} (e.g. B98090-15b supplemental material) and OH stretching at about 3638 cm^{-1} .

173 One of these phyllosilicates, exposed by focussed ion beam milling, was analyzed by
174 energy dispersive X-ray analysis (Anderson and McCarron 2011). These spectra reveal only Al,
175 Si and O, and the Al counts are consistently greater than Si, which is consistent with either
176 cookeite or donbassite.

177 **IMPLICATIONS**

178 The discussion above indicates that the evidence presented in the original description of
179 diomignite is circumstantial, incorrect, or equivocal, and is insufficient to warrant mineral
180 species status. Because: 1) the type material was improperly designated, 2) true type material
181 does not exist, and 3) a neotype sample was not furnished, the identity of the mineral described
182 by London et al. (1987) could not be validated. The discreditation of diomignite, which was
183 approved by the IMA Commission on New Minerals, Nomenclature and Classification, has
184 significant implications for the interpretation of the crystal-rich inclusions in petalite and

185 spodumene and the model proposed by London (2008) for the internal evolution of the Tanco
186 pegmatite.

187 The Tanco pegmatite is among the largest and most highly-evolved pegmatites known
188 and has been the subject of numerous studies over the past 57 years (e.g., Hutchinson 1959;
189 Wright 1963; Crouse and Černý 1972; Černý 2005). The model proposed by London (2008) to
190 explain the cooling history and internal evolution of the Tanco pegmatite is based on fluid
191 inclusion, phase equilibrium, and experimental studies (London 1986; Morgan and London
192 1987; London 2008; London 2015). However, the misidentification of diomignite as a major
193 component in petalite- and spodumene-hosted inclusions negates the existence of a $\text{Li}_2\text{B}_4\text{O}_7$ -
194 flux-rich silicate melt and its possible role in the primary crystallization of the Tanco pegmatite
195 as described by London (2008, 2009).

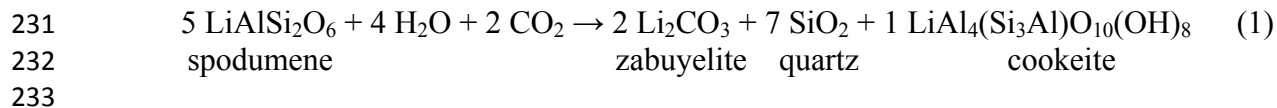
196 According to London (1987) “*Diomignite and the associated aluminosilicate daughter*
197 *minerals represent the crystallization products of a late-stage hydrous borosilicate fluid that was*
198 *entrapped principally by spodumene that formed as a result of the breakdown of petalite to*
199 *spodumene + quartz.*” These same crystal-rich inclusions were later reinterpreted to represent
200 aliquots of flux-rich (12 mass% B_2O_3) boundary layer melt, whose composition is essentially
201 identical to experimentally generated boron-rich (> 10 mass% B_2O_3) boundary layers (London
202 2005, 2008).

203 The name diomignite was derived by London et al. (1987) from Homeric Greek *dios*
204 *mignen*, meaning divine mix, in allusion to the fluxing properties of $\text{Li}_2\text{B}_4\text{O}_7$ on silicate-water
205 systems. The total absence of diomignite in spodumene- and petalite-hosted inclusions,
206 however, refutes the purported role of $\text{Li}_2\text{B}_4\text{O}_7$ in dramatic lowering of solidus temperatures,
207 increasing silicate- H_2O miscibility, and enhancing the solubility of ore-forming incompatible

208 lithophile elements in the Tanco pegmatite (London 1986). Boron in the form of boric acid is
209 enriched in some aqueous fluid inclusions in quartz found within the core of the Tanco
210 pegmatite, and some of these inclusions may contain sassolite (H_3BO_3) daughter crystals
211 (Thomas and Davidson 2015, Rainer Thomas pers. comm. 2015). Similar boron-bearing
212 aqueous fluid inclusions are reported in tourmaline-bearing pegmatites (Williams and Taylor
213 1996; Smirnov et al. 2000; Peretyazhko et al. 2000; Bakker and Schilli 2016) and are generally
214 interpreted to represent aqueous fluids that exsolved from the highly-evolved pegmatite melt
215 during late stage crystallization. London (1985) argued that quartz-hosted aqueous and aqueous
216 carbonic fluid inclusions in the Tanco are secondary in origin and are not representative of the
217 medium from which the quartz was deposited. If this is correct, then the sassolite-bearing fluid
218 inclusions in the quartz core do not represent a flux-rich melt. Furthermore, sassolite is not
219 found within spodumene- or quartz-hosted inclusions in the intermediate zones in the Tanco
220 pegmatite, and the typical concentration of boron in these inclusions is generally less than 1,000
221 ppm (Channer and Spooner 1992; Anderson et al. 2001; Paslawski et al. 2016). These results
222 question whether the crystal-rich inclusions in spodumene are flux-rich at all, and whether they
223 actually represent the crystallized products of a trapped boundary layer melt.

224 Anderson (2013) has pointed out that *secondary* spodumene, formed by the isochemical
225 breakdown of petalite, could not have trapped a boundary layer liquid that is spatially and
226 temporally confined to crystal growth fronts during *primary* crystallization of the pegmatite.

227 It is suggested that the mineral assemblage within these inclusions, consisting of quartz, cookeite
228 and zabuyelite (see supplemental material), formed from of a reaction (1) involving spodumene
229 and an aqueous-carbonic fluid and therefore does not represent the crystallization products of a
230 boron-rich hydrosilicate melt that was trapped during the primary crystal growth.



234 Although laser ablation ICP-MS analyses (Paslawski et al. 2016) show a range of boron
235 concentrations in spodumene-hosted inclusions that is similar to the boron concentrations
236 reported for quartz-hosted inclusions in the intermediate zones at Tanco (Channer and Spooner
237 1992), quantitative analysis of other solutes (e.g., Na, K, Rb, Cs, Sr, Ca, As, Sb) in spodumene-
238 and quartz-hosted inclusions must be determined to ascertain whether or not the same fluid is
239 represented as inclusions in both minerals.

240 ACKNOWLEDGMENTS

241 This work was funded through a NSERC discovery grant to A.J.A. The Smithsonian
242 National Museum of Natural History and the American Museum of Natural History are thanked
243 for loan of the samples designated as the type specimens of diomignite. I am grateful to Petr
244 Černý for providing some of the lithium aluminosilicate samples used in this study. Jacob
245 Hanley is thanked for sharing his Raman microprobe facility, and Thomas Lee helped with the
246 preparation of the figures. Edward S. Grew, Robert M. Hazen, William B. Simmons, Ian
247 Swainson, Dmytro Trots, and an anonymous reviewer are thanked for their useful comments and
248 editorial scrutiny.

249 REFERENCES CITED

- 250 Anderson, A.J. (2013) Are silicate-rich inclusions in spodumene crystallized aliquots of
251 boundary layer melt? *Geofluids*, 13, 460-466.
- 252 Anderson, A.J., and McCarron, T. (2011) Three dimensional textural and chemical
253 characterization of polyphase inclusions in spodumene using a dual focused ion beam-
254 scanning electron microscope (FIB-SEM). *The Canadian Mineralogist*, 49, 541-53.

- 255 Anderson, A.J., Clark, A.H., and Gray, S. (2001) The occurrence and origin of zabuyelite
256 (Li_2CO_3) in spodumene-hosted fluid inclusions: implications for the internal evolution of
257 rare-element granitic pegmatites. *Canadian Mineralogist*, 39, 1513-1527.
- 258
- 259 Bakker, R.J., and Schilli, S.E. (2016) Formation conditions of leucogranite dykes and aplite-
260 pegmatite dykes in the eastern Mt. Capanne plutonic complex (Elba, Italy): fluid inclusion
261 studies in quartz, tourmaline, andalusite and plagioclase. *Mineralogy and Petrology*, 110,
262 43-63.
- 263 Bodnar, R.J. and Student, J.J. (2006) Melt inclusions in plutonic rocks: petrography and
264 microthermometry. In J.D. Webster Ed., *Melt Inclusions in Plutonic Rocks*. Mineralogical
265 Association of the Canada Short Course, 36, p. 1-26.
- 266 Burak, Ya.V., Adamiv, V.T. and Teslyuk, I.M. (2006) To the origin of vibrational modes in
267 Raman spectra of $\text{Li}_2\text{B}_4\text{O}_7$ single crystals. *Functional Materials*, 13, 591-595.
- 268 Černý, P. (2005) The Tanco rare-element pegmatite deposit, Manitoba: regional context, internal
269 anatomy and global comparisons. In R. Linnen and I. Samson, eds., *Rare-Element
270 Geochemistry of Ore Deposits*, Geological Association of Canada, Short Course
271 Handbook, 17, 127-158.
- 272 Channer, D.M.DER. and Spooner, E.T.C. (1992) Analysis of fluid inclusion leachates from
273 quartz by ion chromatography. *Geochimica et Cosmochimica Acta*, 56, 249-259.
- 274 Crouse, R.A., and Černý, P. (1972) The Tanco pegmatite at Bernic Lake, Manitoba. I *Geology
275 and paragenesis*. *The Canadian Mineralogist*, 11, 591-608.
- 276 Dowty, E. (2000): *SHAPE for Windows, Version 6*, Shape Software.
- 277 Dukelski, M. (1906) Über Borate. *Zeitschrift für anorganische Chemie*, 50, 38-48.

- 278 Gorelik, V.S., Vdovin, A.V., and Moiseenko, V.N. (2003) Raman and hyper-Rayleigh scattering
279 in lithium tetraborate crystals. *Journal of Russian Laser Research*, 24, 553-605.
- 280 Hålenius, U., Hatert, F., Pasero, M., and Mills, S.J. (2016) New minerals and nomenclature
281 modifications approved in 2015 and 2016. *Mineralogical Magazine*, 80(1), 199-205.
- 282 Hutchinson, R.W. (1959) Geology of the Montgary pegmatite. *Economic Geology*, 54, 1525-
283 1542.
- 284 London, D. (1985) Origin and significance of inclusions in quartz: a cautionary example from
285 the Tanco pegmatite, Manitoba. *Economic Geology*, 80, 1988-1995.
- 286 London, D. (1986) Magmatic-hydrothermal transition in the Tanco rare-element pegmatite:
287 evidence from fluid inclusions and phase equilibrium experiments. *American*
288 *Mineralogist*, 71, 376-395.
- 289 London, D. (2005) Granitic pegmatites: an assessment of current concepts and directions for the
290 future. *Lithos*, 80, 281-303.
- 291 London, D. (2008) Pegmatites. *The Canadian Mineralogist*, Special Publication, 10, 347 p.
- 292 London, D. (2009) The origin of primary textures in granitic pegmatites. *The Canadian*
293 *Mineralogist*, 47, 697-724.
- 294 London, D. (2015) Reply to Thomas and Davidson on “A petrologic assessment of internal
295 zonation in granitic pegmatites” (London 2014a). *Lithos*, 212-215, 469-484.
- 296 London, D., Zolensky, M.E., and Roedder, E. (1987) Diomignite: natural $\text{Li}_2\text{B}_4\text{O}_7$ from the
297 Tanco pegmatite, Bernic Lake, Manitoba. *The Canadian Mineralogist*, 25, 173-80.
- 298 Morgan, G.B., VI, and London, D. (1987) Alteration of amphibolitic wallrocks around the Tanco
299 rare-element pegmatite, Bernic Lake, Manitoba. *American Mineralogist*, 72, 1097-1121.

- 300 Paslawski, L., Anderson A.J., MacFarlane, C., and Boucher, B. (2016) Boron concentrations in
301 spodumene-hosted fluid inclusions from the Tanco pegmatite, Manitoba, Canada. 42nd
302 Colloquium and Annual Meeting of the Atlantic Geoscience Society, Truro, Nova Scotia,
303 (Abstract), *Atlantic Geology*, 52, 89-90.
- 304 Paul, G.L., and Taylor, W. (1982) Raman spectrum of $\text{Li}_2\text{B}_4\text{O}_7$. *Journal of Physics C: Solid State*
305 *Physics*. 15, 1753-1764.
- 306 Peretyazhko, I.S., Prokof'ev, V.Y., Zagorskii, V.E., and Smirnov, S.Z. (2000) Role of boric acids
307 in the formation of pegmatite and hydrothermal minerals: petrologic consequences of
308 sassolite (H_3BO_3) discovery in fluid inclusions. *Petrology*, 8, 214-237.
- 309 Reburn, W.T., and Gale, W.A. (1955) The system lithium oxide - boric oxide - water. *Journal of*
310 *Physical Chemistry*, 59, 19-24.
- 311 Rosasco, G.J., and Roedder, E. (1979) Application of a new Raman microprobe spectrometer to
312 nondestructive analysis of sulfate and other ions in individual phases in fluid inclusions in
313 minerals. *Geochimica et Cosmochimica Acta*, 43, 1907-1915.
- 314 Smirnov, S.Z., Peretyazhko, I.S., Zagorskii, V.E., and Shebanin, A.P. (2000) The first finding of
315 sassolite (H_3BO_3) in fluid inclusions in minerals. *Russian Geology and Geophysics*, 41 (2),
316 193-205.
- 317 Thomas, R., and Davidson, P. (2010) Hambergite-rich melt inclusions in morganite crystals from
318 the Muiane pegmatite, Mozambique and some remarks on the paragenesis of hambergite.
319 *Mineralogy and Petrology*, 100, 227-239.
- 320 Thomas, R., and Davidson, P. (2015) Comment on "A petrologic assessment of internal zonation
321 in granitic pegmatites" by David London (2014). *Lithos*, 212-215, 462-468.

- 322 Touboul, M., and Bétourné, E. (1996) Dehydration process of lithium borates. *Solid State Ionics*,
323 84, 189-197.
- 324 Wan, S., Tang, X., Sun, Y., Zhang, G., You, J., and Fu, P. (2014) Raman spectroscopy and
325 density functional theory analysis of the melt structure in a $\text{Li}_2\text{B}_4\text{O}_7$ crystal growth system.
326 *CrystEngComm*, 16, 3086-3090.
- 327 Williams, A.E., and Taylor, M. (1996) Mass spectrometric identification of boric acid in fluid
328 inclusions in pegmatite minerals. *Geochimica et Cosmochimica Acta*, 60, 3435-3443.
- 329 Wright, C.M. (1963) Geology and origin of the pollucite-bearing Montgary pegmatite, Manitoba.
330 *Geological Association of America Bulletin*, 74, 919-946.

331

332

LIST OF FIGURES

333

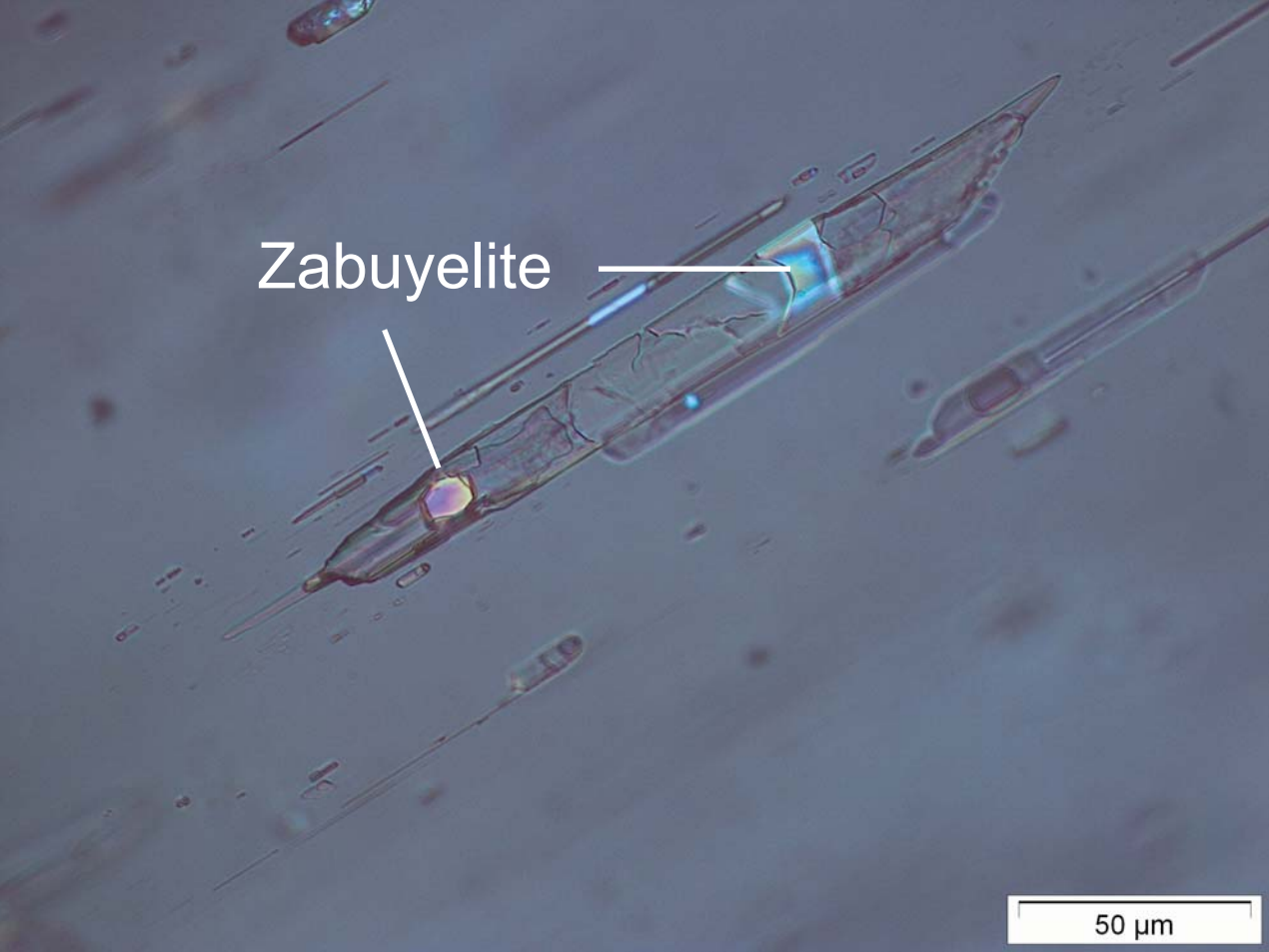
334 Figure 1: Photomicrograph of a spodumene-hosted inclusion in the type sample AMNH 98090
335 viewed under crossed polarized light. The inclusion contains two high-birefringence zabuyelite
336 crystals that display different relief and retardation due to differences in size and orientation.

337 Figure 2: (a) Pseudo-cubic outline of zabuyelite when viewed down the c-axis. (b) Pseudo-
338 hexagonal outline of zabuyelite when viewed down the c-axis.

339

Zabuyelite

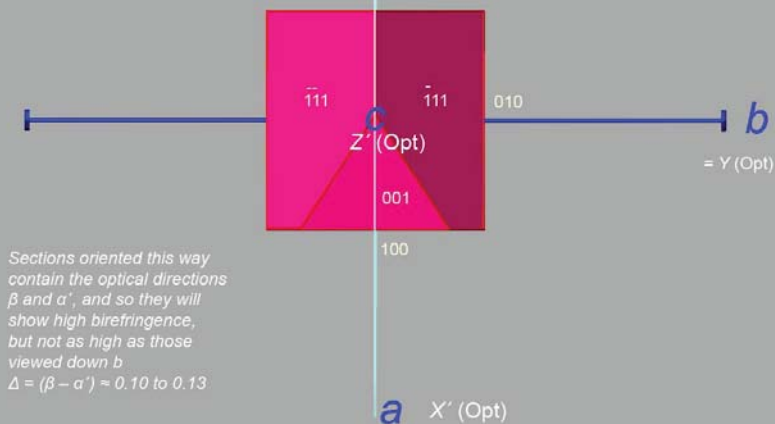
50 μm



(a) Zabuyelite

orthogonal, pseudo-cubic outline

- faces $(-1-11)$, (-111) and (001) have been left for comparison to pseudo-hexagonal drawing



(b) Zabuyelite

pseudo-hexagonal outline (interfacial angles of 57 and 66 degrees)

- notice the prominent, triangular (001) face

